

See discussions, stats, and author profiles for this publication at: <https://www.researchgate.net/publication/263704242>

# Superomniphobic, Transparent, and Antireflection Surfaces Based on Hierarchical Nanostructures

ARTICLE *in* NANO LETTERS · JULY 2014

Impact Factor: 13.59 · DOI: 10.1021/nl501767j · Source: PubMed

---

CITATIONS

6

READS

64

## 8 AUTHORS, INCLUDING:



Prantik Mazumder

Corning Incorporated

24 PUBLICATIONS 226 CITATIONS

[SEE PROFILE](#)



Yongdong Jiang

nGimat Co.

17 PUBLICATIONS 367 CITATIONS

[SEE PROFILE](#)



Domenico Tulli

DAS Photonics SL

20 PUBLICATIONS 76 CITATIONS

[SEE PROFILE](#)



Daniel Infante

École Polytechnique Fédérale de Lausanne

5 PUBLICATIONS 20 CITATIONS

[SEE PROFILE](#)

# Superomniphobic, Transparent, and Antireflection Surfaces Based on Hierarchical Nanostructures

Prantik Mazumder,<sup>\*,†</sup> Yongdong Jiang,<sup>‡</sup> David Baker,<sup>†</sup> Albert Carrilero,<sup>§</sup> Domenico Tulli,<sup>§,⊥</sup> Daniel Infante,<sup>§,#</sup> Andrew T. Hunt,<sup>‡</sup> and Valerio Pruneri<sup>\*,§,||</sup>

<sup>†</sup>Corning Incorporated, Sullivan Park, Corning, New York 14831, United States

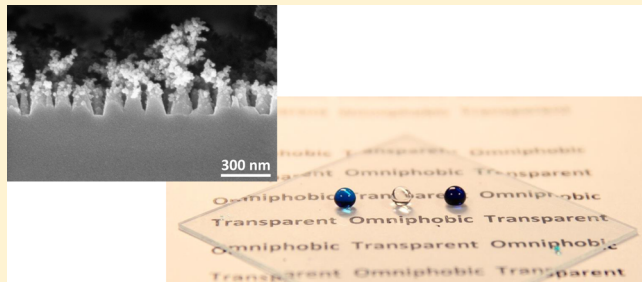
<sup>‡</sup>nGimat Co., 1824 Willow Trail Parkway, Norcross, Georgia 30093, United States

<sup>§</sup>ICFO—Institut de Ciències Fotòniques, Av. Carl Friedrich Gauss, 3, 08860 Castelldefels, Barcelona, Spain

<sup>||</sup>ICREA—Institució Catalana de Recerca i Estudis Avançats, Passeig Lluís Companys, 23, 08010 Barcelona, Spain

**ABSTRACT:** Optical surfaces that can repel both water and oil have much potential for applications in a diverse array of technologies including self-cleaning solar panels, anti-icing windows and windshields for automobiles and aircrafts, low-drag surfaces, and antismudge touch screens. By exploiting a hierarchical geometry made of two-tier nanostructures, primary nanopillars of length scale  $\sim$ 100–200 nm superposed with secondary branching nanostructures made of nanoparticles of length scale  $\sim$ 10–30 nm, we have achieved static contact angles of more than  $170^\circ$  and  $160^\circ$  for water and oil, respectively, while the sliding angles were lower than  $4^\circ$ . At the same time, with respect to the initial flat bare glass, the nanotextured surface presented significantly reduced reflection (<0.5%), increased transmission (93.8% average over the 400 to 700 nm wavelength range), and very low scattering values (about 1% haze). To the authors' knowledge, these are the highest optical performances in conjunction with superomniphobicity reported to date in the literature. The primary nanopillars are monolithically integrated in the glass surface using lithography-free metal dewetting followed by reactive ion etching,<sup>1</sup> while the smaller and higher surface area branching structure made of secondary nanoparticles are deposited by the NanoSpray<sup>2</sup> combustion chemical vapor deposition (CCVD).

**KEYWORDS:** Nanostructured optical surfaces, superomniphobic surfaces, self-cleaning, transparent surfaces



Transparent, superomniphobic surfaces that can repel both water and oil are in demand due to various potential applications. Superhydrophobic surfaces with a water contact angle greater than  $150^\circ$  can be achieved by creating rough structures coated with fluorinated materials. Various combinations of materials and processing routes to produce superhydrophobic surfaces have been reported in the literature.<sup>3–7</sup> Few also made inroad into commercial markets such as NeverWet, P2i,<sup>8</sup> and Liquipel<sup>9</sup> technologies. In contrast, developing superoleophobic surface on which the contact angle of oil or other organic liquids is greater than  $150^\circ$  remains much more challenging.<sup>10–13</sup> This is due to the fact that the surface tensions of oil and other organic liquids are very low and therefore spontaneously spread on most solid surfaces. For example, the surface tension of water is 73 dyn/cm, whereas that of hexadecane is only 27.7 dyn/cm. Therefore, the latter has more propensities to completely wet a solid surface with high surface energy. The wettability of a solid surface, however, can be modified by surface chemistry or surface roughness or a combination of both. A liquid droplet on a rough surface can assume one of two equilibrium states: the Wenzel state or the Cassie–Baxter state.<sup>3,14,15</sup> In the Wenzel state, the liquid fully wets the solid surface and therefore, there is an increase in the

true area of contact between the liquid and the solid. This, in turn, amplifies the wetting or nonwetting property of the surface. The apparent contact angle  $\theta_W$  in this configuration is given by  $\cos \theta_W = r \cos \theta_Y$ , where the surface roughness factor  $r$  is defined as the actual surface area divided by the projected surface area and  $\theta_Y$  is the Young's contact angle measured on a smooth surface with same surface chemistry as the textured surface.<sup>12</sup> If the Young's contact angle of the liquid is less than  $90^\circ$ , the contact angle in the Wenzel state will be even lower than the Young contact angle. However, if the Young's contact angle is greater than  $90^\circ$ , the contact angle in the Wenzel state will be greater than the Young contact angle. Since the water contact angle is  $\sim$ 110° on a flat surface coated with a fluoropolymer, a superhydrophobic surface in Wenzel state is possible.<sup>13–16</sup> However, since the Young's contact angle for oil and other organic liquids are less than  $90^\circ$  on any flat surface, even when it is coated with fluoropolymers, oleophobility is not possible in the Wenzel state, let alone superoleophobicity. In the Cassie–Baxter state, a composite solid–liquid–air

**Received:** May 12, 2014

**Revised:** June 29, 2014

**Published:** July 2, 2014

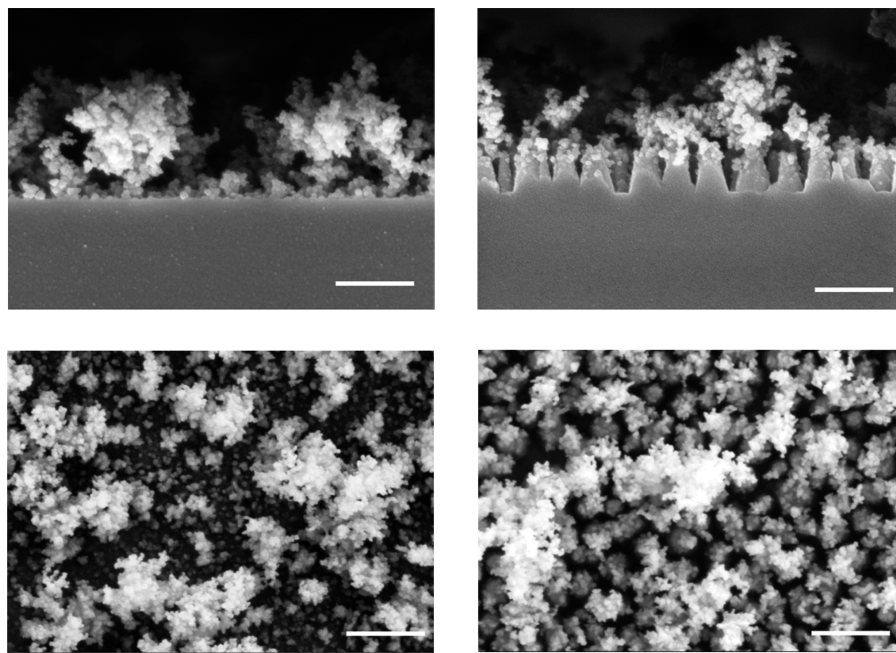


**Figure 1.** SEM of branching nanostructures on flat surface (left) and on the nanopillars (right): cross sections (top) and top views (bottom). The scale bar represents 300 nm.

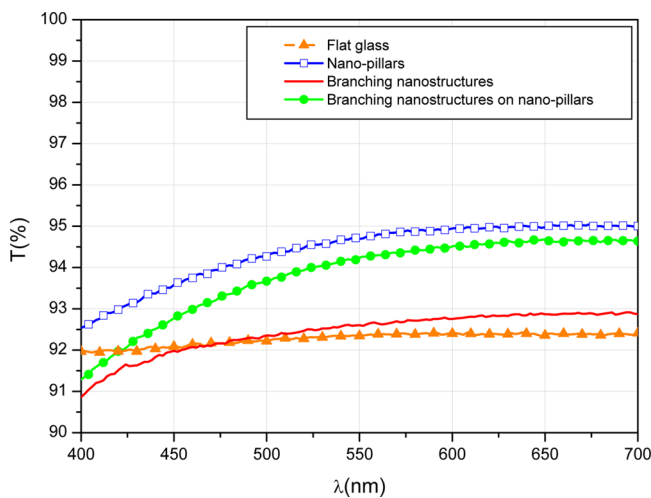


**Figure 2.** Direct optical transmission as a function of wavelength. The antireflection effect and corresponding change in transmission of the nanostructuring of one of the two surfaces are clearly visible.

**Table 1. Contact Angles in Degrees before and after the Branching Nanostructures, and Low Surface Tension Monolayer Fluorosilane Is Applied to the Flat and Nanopillar Corning Glass Substrates**

	water (72.1 mN/m)	oleic acid (32.9 mN/m)	hexadecane (27.7 mN/m)
flat glass	113 ± 3	78 ± 2	67 ± 2
nanopillars	144 ± 4	118 ± 2	104 ± 3
branching nanostructures	165 ± 3	157 ± 3	150 ± 3
branching nanostructures on nanopillars	172 ± 4	163 ± 3	153 ± 3

interface develops, where air is trapped underneath the liquid.<sup>3,10–13</sup> Thus, there is a reduction in true area of contact between the liquid and the solid and a significant area of the liquid meniscus could be suspended in air. The apparent

contact angle  $\theta_{CB}$  is given by  $\cos \theta_{CB} = -1 + f(1 + r_f \cos \theta_Y)$  where  $r_f$  is the roughness factor of the wetted area and  $f$  is the fraction of the projected area of the solid surface under the drop that is wetted by the liquid.<sup>17,18</sup> By decreasing the liquid–solid fraction of the meniscus area,  $f$ , one could achieve very high oil contact angle. However, the Cassie–Baxter state for oil or any liquid with Young contact angle lower than 90 deg is thermodynamically unstable compared to its Wenzel state. The free energy of the latter is always lower than the former for these liquids.<sup>4</sup> Several studies have shown that specific geometries, such as overhang or re-entrant structures, can offer meta-stability to the Cassie–Baxter state by creating local energy barriers.<sup>6,12,19,20,22–24</sup> It has been generally accepted that in order to create a stable superomniphobic state, re-entrant or hierarchical geometry is necessary.<sup>10,11</sup> Many examples of such structures made by various processing techniques have been reported in the literature.<sup>10–12,19,20</sup> In addition to superomniphobicity, if the surface were to be optically transparent, the physical dimensions of the hierarchical structures must be smaller than the wavelength of visible light.<sup>21</sup> Thus, all the length scales must be less than 300 nm or even smaller. Recently, a superomniphobic coating made of porous carbon candle soot coated with nanometer silica shells has been achieved on flat glass, with extraordinary contact angles for water and hexadecane of about 165° and 156° and roll-off (sliding) angles less than 5°.<sup>24</sup> After calcination at 600 °C the coating becomes transparent. However, the superoleophobicity is only achieved when the soot thickness is greater than 2 μm. As a result, the optical transmission is rather poor with respect to the initial glass substrate (at 400 nm the optical transmission is about 70%) for such thick soot coating. In addition, the strong monotonic decrease of transmission with decreasing wavelength in their data is a sign of significant scattering (or haze). However, the high transmission (>90%) is only attained when the soot thickness is smaller than one micron for which the oil contact angle is not high enough to be superoleophobic. To the best of our knowledge, a surface with optical

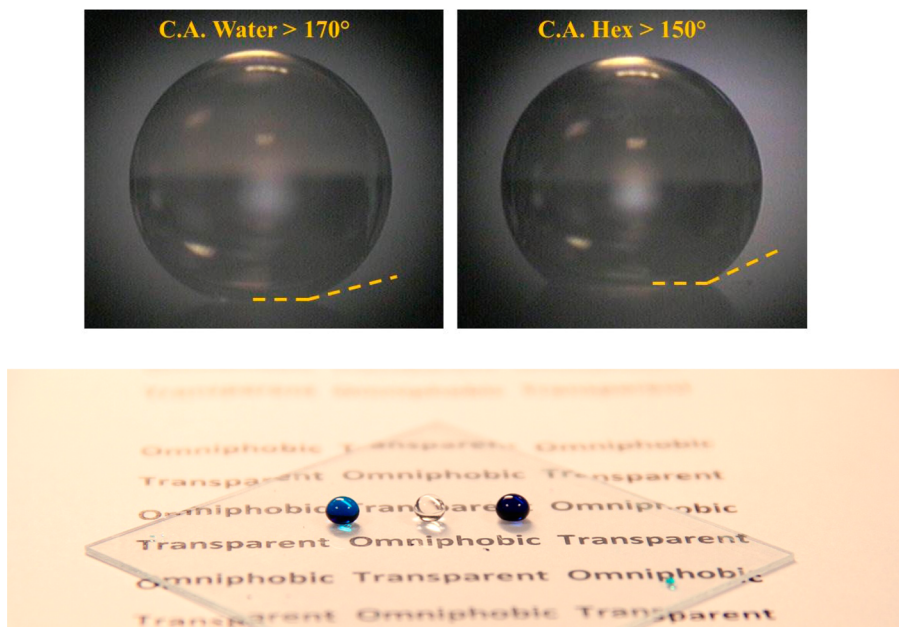


**Figure 3.** Wetting of branching nanostructures on nanopillar substrate after application of fluorosilane: water and hexadecane droplets with contact angle of  $>170^\circ$  and  $150^\circ$ , respectively (top), and image with three liquid droplets of different surface tension: water (bottom middle), oleic acid (bottom left), and hexadecane (bottom right).

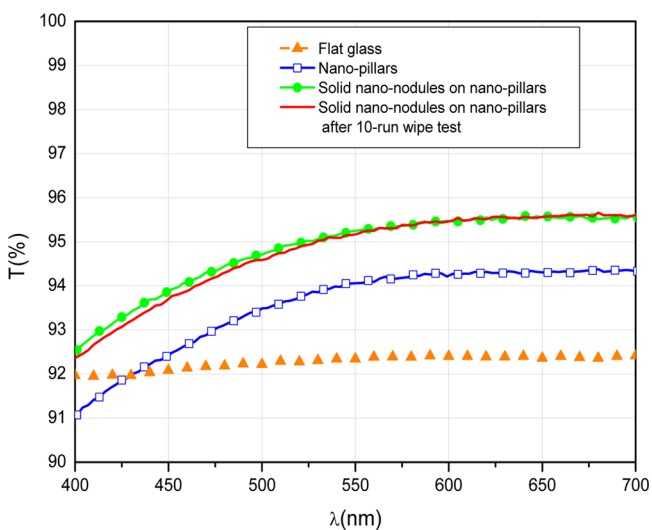
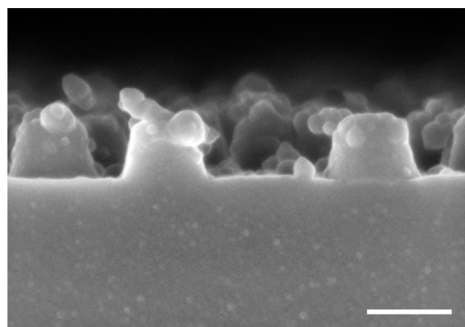


**Figure 4.** Durable hierarchical nanostructure. Top: solid nanonodules on nanopillars (scale bar is 200 nm). Bottom: measured direct spectral transmittance showing the improvements due to primary nanopillars, secondary nanonodules on nanopillars, and resistance against rubbing of the hierarchical structure (nanonodules on nanopillars).

transmission greater than  $>90\%$  and oil contact angle greater than  $>150^\circ$  has never been reported. In this letter, we report a nanotextured glass surface with high transmission, low haze, and superomniphobic properties. Hierarchical structure is made of primary nanopillars and secondary branching nanostructures. The initial hydrophobic and oleophobic properties of the primary nanopillar structure were further increased by the branching nanostructures. Branching nanostructures of small thicknesses could then be used, and this, combined with the antireflection property of the nanopillars,<sup>25</sup> produced high optical transmission and low haze. We were able to produce surfaces with contact angles of more than  $170^\circ$ ,  $160^\circ$ , and  $150^\circ$  for water, oleic acid, and hexadecane, respectively. The surface also showed very low contact line pinning or hysteresis, very high optical transmission of about 94% (average value over the visible), and very low haze of about 1%.

**Methods.** The primary nanopillars on the glass surface are fabricated by creating nanoscale metal masks on glass followed by reactive ion etching of the latter. Ultrathin metal films are first deposited on the flat glass surface. In a subsequent and rapid thermal annealing step the metal film is dewetted into discrete nanoparticles. These metal nanoparticles are subsequently used as masks during reactive ion etching of the surface. After removal of the metal masks, the surface is covered by monolithically integrated nanopillars whose geometry could be controlled by the process conditions. Details of the process could be found in a separate reference.<sup>1</sup> Two types of secondary nanostructures, branching nanostructures and nanonodules, were deposited on the primary nanopillars by the NanoSpray CCVD process using the proprietary Nanomiser<sup>2</sup> device. The structures were controlled by the process conditions such as solution concentration, composition, and deposition temperature.<sup>26,27</sup>

All the nanostructures were treated with a low surface energy fluorosilane. The glass samples were placed in a fluorosilane solution for a certain period of time followed by rinsing by a solvent and deionized water and drying in nitrogen. The CCVD

coatings do not wash off during the above-mentioned processing, which suggests strong adhesion between the secondary nanostructures and the glass surface underneath. The total (i.e., specular and diffuse) transmittance and reflectance were measured in the wavelength range of 390 to 800 nm by using a UV-vis-NIR spectrophotometer (PerkinElmer Lambda 950). Haze was measured by using a Haze-meter (BYK-Gardner 4601 haze-gloss). Water, oleic acid, and hexadecane contact angles were measured and averaged at three different positions on the surface of samples by using a drop shape analysis system (DSA-100, Krüss GmbH).

**Experimental Results.** Figure 1 shows the typical nanostructures on Corning glass substrates. The thickness of the highly porous silica branching nanostructures is of the order of a few hundreds of nanometers, while the height and the average diameter of the primary nanopillars are  $\sim 200$  and  $\sim 100$  nm, respectively. We have also estimated that the percentage coverage, i.e., ratio between area covered by the nanopillars and total area, varies between 20 and 25%. By comparing the top views (bottom pictures in Figure 1), one can appreciate that the branching nanostructures are more uniform on the nanopillars than on the bare sections of the flat surface. This is likely due to the fact that it preferentially grows on the (top-right figure) nanopillars.

Figure 2 shows the optical transmission as a function of wavelength, for flat glass substrate, substrates with only primary nanopillar, substrates with only branching nanostructures, and substrates with primary nanopillars superposed with branching nanostructures. One can appreciate the antireflection (AR) property of the nanopillars: the 4% reflection from the flat surfaces is reduced to practically negligible values (below 0.5%) in the presence of the nanopillars. Note that the nanostructure is applied to only one surface of the substrate, while the optical transmission in the graph also includes (i.e., it is reduced) the reflection from the back, always flat, surface. As a result, the average transmission over the 400 to 700 nm range increases from 92.2% (flat) to 94.4% (nanopillars). This is accompanied by an increase of haze, from 0.2 (flat) to 0.8%. When one applies the branching nanostructures on the flat surface, the AR effect is much smaller than that of the nanopillars, ending with a similar average transmission (92.42%) to flat glass and with a haze of 1.6%. At optimized conditions, the CCVD coatings have achieved a haze of less than 1% and more than 50% reduction in reflection from flat glass surface. In any case, the branching nanostructures present a transmission loss much smaller than that of previous works (for example, ref 10.). When the branching nanostructures are superimposed on the nanopillar substrate, one can obtain an average transmission of 93.82% and a haze of 1.2%. Note that the scattering of the combined nanopillar and branching structure is lower than that of the branching nanostructures alone, possibly because the nanopillars seed the branching growth and provides a more uniform distribution of the nanoparticles over the substrate. The reduced reflection is because of the lowered refractive index of the nanopillar/nanobranching structure due to their porous character.

Table 1 summarizes the contact angles measured on flat and nanostructured surfaces after applying a fluorosilane self-assembled monolayer coating. The Young contact angles of water, oleic acid, and hexadecane on flat glass surface are  $113^\circ \pm 3$ ,  $78^\circ \pm 2$ , and  $67^\circ \pm 2$ , respectively. The contact angles are  $144^\circ \pm 4$ ,  $118^\circ \pm 2$ , and  $104^\circ \pm 3$ , respectively, on the substrate with only primary nanopillars. The contact angles on

substrates with only nanobranching structures are  $165^\circ \pm 3$ ,  $157^\circ \pm 3$ , and  $150^\circ \pm 3$ . Finally, the contact angles of  $172^\circ \pm 4$ ,  $163^\circ \pm 3$ , and  $153^\circ \pm 2$  are obtained on the substrate with primary nanopillars superposed with secondary nanobranching structures. To the best of our knowledge, this is the first such combination of superoleophobicity (Hexadecane CA >  $150^\circ$ ) and high transmission (>92%). The improvement when one uses a substrate with nanopillars rather than a flat one is also significant if one considers the fact that starting contact angles are already very high. The rolling angles for the different liquids on both the hierarchical branching nanostructures on nanopillar and branching nanostructures on flat surfaces are similar, increasing from water ( $<3^\circ$ ) to oleic acid ( $<4^\circ$ ) and hexadecane ( $<6^\circ$ ). Figure 3 shows the water, oil, and hexadecane droplets on the hierarchical branching nanostructures on the nanopillar surface, where one can appreciate visually the angles reported in Table 1. Note that samples of different nanopillars and branching nanostructures varying in dimensions within  $\pm 15\%$  produced similar results.

Although optical and wetting properties of these highly porous coatings are extremely high, when mechanical abrasion is applied they suffer from the fragility of the porous branching nanostructures. For this reason, we have also investigated solid nanonodules with an average diameter between 25 and 50 nm, which form clusters on the glass surface covered by primary nanopillars (Figure 4 top). This hierarchical structure allows a high optical transmission, averaging 95% in the 400–700 nm range (Figure 4 bottom). The robustness of this structure is improved with respect to the branching nanostructure. After a 10 run wipe test, optical transmission and haze remain approximately the same (see Figure 4), indicating that the nanopillars not only help to increase transparency but also may have protected the nanonodules. The contact angles for the liquid tested are only slightly higher (between 5 and  $10^\circ$ ) than the initial primary nanopillars (see Table 1) indicating that in this case the secondary structure is not as efficient as the branching nanostructures. The future optimization of the proposed structures should lead to a proper trade-off between wetting, optical, and mechanical durability performance.

**Conclusions.** A transparent antireflection glass substrate with superomniphobic properties has been achieved by surface nanostructuring. Record optical transmission and haze (scattering) values in conjunction with very large water and oil contact angles are reported for a hierarchical structure made of primary nanopillars and secondary branching nanostructures, obtained by metal dewetting/etching and NanoSpray CCVD techniques, respectively. The proposed design and methods can lead to surfaces for a wide range of applications, such as self-cleaning solar panels, anti-icing car and aircraft windshields, and antimudge touch screens.

## ■ AUTHOR INFORMATION

### Corresponding Authors

\*(V.P.) E-mail: valerio.pruneri@icfo.es.

\*(P.M.) E-mail: mazumderp@corning.com.

### Present Addresses

<sup>†</sup>(D.T.) Department of Electrical and Computer Engineering, University of California, Davis, California 95616, United States.

<sup>#</sup>(D.I.) Optics & Photonics Technology Laboratory, École Polytechnique Fédérale de Lausanne (EPFL), Rue de la Maladière 71b, 2000 Neuchâtel, Switzerland.

## Notes

The authors declare no competing financial interest.

## ■ REFERENCES

- (1) Infante, D.; Koch, K. W.; Mazumder, P.; Tian, L.; Carrilero, A.; Tulli, D.; Baker, D.; Pruneri, V. Durable, Superhydrophobic, Antireflection and Low Haze Glass Surfaces Using Scalable Metal Dewetting Nanostructuring. *Nano Res.* **2013**, *6*, 429–440.
- (2) Jiang, Y.; White, M.; Venugopal, G.; Hunt, A. T. Development and Commercialization of Nanomaterials by the NanoSpray<sup>SM</sup> Combustion Processing Technology. *MRS Proc.* **2013**, 1533.
- (3) Feng, L.; Li, S.; Li, Y.; Li, H.; Zhang, L.; Zhai, J.; Song, Y.; Liu, B.; Jiang, L.; Zhu, D. Super-Hydrophobic Surfaces: from Natural to Artificial. *Adv. Mater.* **2002**, *24*, 1857–1860.
- (4) Patankar, N. A. Mimicking the Lotus Effect: Influence of Double Roughness Structures and Slender Pillars. *Langmuir* **2004**, *20*, 8209–8213.
- (5) Marmur, A. From Hygrophilic to Superhydrophobic: Theoretical Conditions for Making High-Contact-Angle Surfaces from Low-Contact-Angle Materials. *Langmuir* **2008**, *24*, 7573–7579.
- (6) Nosonovsky, M.; Bhushan, B. Biomimetic Superhydrophobic Surfaces: Multiscale Approach. *Nano Lett.* **2007**, *7*, 2633–2637.
- (7) Kwon, Y.; Patankar, N.; Choi, J.; Lee, J. Design of Surface Hierarchy for Extreme Hydrophobicity. *Langmuir* **2009**, *25*, 6129–6136.
- (8) Badyal, J. P. S.; Coulson, S. R.; Willis C. R. Surface Coatings, US Patent RE43651E, Sept. 11, 2012.
- (9) Legein, F.; Vanlandeghem, A.; Martens, P. Coated electronic devices and associated methods, US Patent 20120296032, Nov. 22, 2012.
- (10) Tuteja, A.; Choi, W.; McKinley, G. H.; Cohen, R. E.; Rubner, M. F. Design Parameters for Superhydrophobicity and Superoleophobicity. *MRS Bull.* **2008**, *33* (8), 752–758.
- (11) Tuteja, A.; Choi, W.; Mabry, J. M.; McKinley, G. H.; Cohen, R. E. Robust Omniphotic Surfaces. *Proc. Natl. Acad. Sci. U.S.A.* **2008**, *105* (47), 18200–18205.
- (12) Callies, M.; Quéré, D. On water repellency. *Soft Matter* **2005**, *1* (1), 55–61.
- (13) Coulson, S. R.; Woodward, I.; Badyal, J. P. S.; Brewer, S. A.; Willis, C. Super-repellent composite fluoropolymer surfaces. *J. Phys. Chem. B* **2000**, *104*, 8836–8840.
- (14) Wenzel, R. N. Resistance of solid surfaces to wetting by water. *Ind. Eng. Chem.* **1936**, *28*, 988–994.
- (15) Cassie, A. B. D.; Baxter, S. Wettability of porous surfaces. *Trans. Faraday Soc.* **1944**, *40*, 546.
- (16) Nishino, T.; Meguro, M.; Nakamae, K.; Matsushita, M.; Ueda, Y. The Lowest Surface Free Energy Based on –CF<sub>3</sub> Alignment. *Langmuir* **1999**, *15*, 4321.
- (17) Marmur, A. Wetting on hydrophobic rough surfaces: To be heterogeneous or not to be? *Langmuir* **2003**, *19*, 8343–8348.
- (18) Michielsen, S.; Lee, H. J. Design of a superhydrophobic surface using woven structures. *Langmuir* **2007**, *23*, 6004–6010.
- (19) Tuteja, A.; Choi, W.; Ma, M.; Mabry, J. M.; Mazzella, S. A.; Rutledge, G. C.; McKinley, G. H.; Cohen, R. E. Designing Superoleophobic Surfaces. *Science* **2007**, *318*, 1618–1622.
- (20) Cao, L.; Price, T. P.; Weiss, M.; Gao, D. Super Water- and Oil-Repellent Surfaces on Intrinsically Hydrophilic and Oleophilic Porous Silicon Films. *Langmuir* **2008**, *24*, 1640–1643.
- (21) Zhang, Y. F.; Li, J. H.; Zhu, S. J.; Dong, H. P.; Jia, F.; Wang, Z. H.; Sun, Z. Q.; Zhang, L.; Li, Y.; Li, H. B.; Xu, W. Q.; Yang, B. Biomimetic Surfaces for High-Performance Optics. *Adv. Mater.* **2009**, *21*, 4731.
- (22) Im, M.; Im, H.; Lee, J. H.; Yoon, J. B.; Choi, Y. K. A Robust Superhydrophobic and Superoleophobic Surface with Inverse-Trapezoidal Microstructures on a Large Transparent Flexible Substrate. *Soft Matter* **2010**, *6*, 1401–1404.
- (23) Tuteja, A.; Choi, W.; Mabry, J. M.; McKinley, G. H.; Cohen, R. E. Transparency and Damage Tolerance of Patternable Omniphotic Lubricated Surfaces Based on Inverse Colloidal Monolayers. *Nat. Commun.* **2013**, *4*, 2167.
- (24) Deng, X.; Mammen, L.; Butt, H.-J.; Vollmer, D. Candle Soot as a Template for a Transparent Robust Superamphiphobic Coating. *Science* **2012**, *335*, 67.
- (25) Moharam, M. G.; Gaylord, T. K. Rigorous Coupled-Wave Analysis for Planar-Grating Diffraction. *J. Opt. Soc. Am.* **1981**, *71* (7), 811–818.
- (26) Hunt, A. T.; Carter, W. B.; Cochran, J. K., Jr. Combustion Chemical Vapor Deposition: a Novel Thin-Film Deposition Technique. *Appl. Phys. Lett.* **1993**, *63* (2), 266–268.
- (27) Alexiou, A. E.; Shanmugham, S.; Hampikian, J. M. The Deposition of Chromia, Chromia/Yttria, and Silica Coatings Via Combustion CVD. In *Elevated Temperature Coatings: Science and Technology III*, Proceedings of a Symposium Held during 1999 TMS Annual Meeting in San Diego, CA, Feb. 28–Mar. 4; Hampikian, J. M., Dahotre, N. B., Eds.; The Minerals, Metals and Materials Society: Warrendale, PA, 1999; pp 329–339.